

- J. Geophys. Res.* **86**, 6261 (1981)]. Basalts on Mars and Mercury are similarly expected to tap source regions as deep as ~250 km, well below the estimated ~100 to 200 km (past to present) thickness of the lithosphere on Mercury [H. J. Melosh and W. B. McKinnon, in (2), p. 374; (7)]. Measurements and estimates of mantle plus crust thicknesses range from 2885 km and 2300 to 2950 km for Earth and Venus to 1250 to 1750 km, 1300 to 2100 km, and 500 to 650 km for the moon, Mars, and Mercury, respectively [A. M. Dziewonski and D. L. Anderson, *Phys. Earth Planet. Inter.* **25**, 297 (1981); (1, 3, 5, 7)].
11. G. W. Wetherill, in (2), p. 670.
 12. W. Benz, W. L. Slattery, A. G. W. Cameron, *Icarus* **74**, 516 (1988); A. G. W. Cameron, B. Fegley Jr., W. Benz, W. L. Slattery, in (2), p. 692.
 13. In particular, we set aside older models that advocate a uniquely refractory-rich composition for Mercury among terrestrial planets [see J. T. Wasson, in (2), p. 622; (3)].
 14. W. B. Tonks and H. J. Melosh, *Icarus* **109**, 326 (1992); J. J. Lissauer and G. R. Stewart, in *Protostars and Planets III*, E. H. Levy and J. I. Lunine, Eds. (Univ. of Arizona Press, Tucson, 1993), p. 1061.
 15. D. L. Mitchell and I. de Pater, *Icarus* **110**, 2 (1994).
 16. M. J. Ledlow *et al.*, *Astrophys. J.* **384**, 640 (1992).
 17. A. R. von Hippel, Ed., *Dielectric Materials and Applications* (MIT Press, Cambridge, MA, 1952). The high dielectric loss is associated with the ferroelectric behavior of the titanate perovskites.
 18. J. T. Wasson, in (2), p. 622; J. S. Lewis, *ibid.*, p. 651.
 19. A. Potter and T. Morgan, *Science* **229**, 651 (1985); *Icarus* **67**, 336 (1986); *Science* **248**, 835 (1990); D. M. Hunten, T. H. Morgan, D. E. Shemansky, in (2), p. 562; A. L. Sprague, R. W. H. Kozlowski, D. M. Hunten, *Science* **249**, 1140 (1990); R. M. Killen, A. E. Potter, T. H. Morgan, *ibid.* **252**, 974 (1991).
 20. G. H. Heiken, D. T. Vaniman, B. M. French, *Lunar Sourcebook* (Cambridge Univ. Press, New York, 1991).
 21. The FeO/MgO molar ratio is enhanced about three- to fivefold in basaltic melt relative to the coexisting peridotitic assemblage of crystals; if we account for the accompanying enrichment in silica, alumina, and other components, the percentage of FeO (by weight) remains constant to within a factor of ~0.5 to 2 between the partial melt and the original source rock [P. L. Roeder and R. F. Emmslie, *Contrib. Mineral. Petrol.* **29**, 275 (1970); (5, 8, 9)].
 22. This conclusion bears on the interpretation of the smooth and intercrater plains of Mercury because their extensive coverage has been a leading argument for their volcanic origin (1). Were these plains primarily basaltic, we would have obtained significantly higher values of dielectric loss than were found (15).
 23. J. Veverka, P. Helfenstein, B. Hapke, J. D. Goguen, in (2), p. 37.
 24. F. Vilas, *ibid.*, p. 59.
 25. A. L. Tyler (Sprague), R. H. W. Kozlowski, L. A. Lebofsky, *Geophys. Res. Lett.* **15**, 808 (1988); A. L. Sprague, R. W. H. Kozlowski, F. C. Witteborn, D. P. Cruikshank, D. H. Wooden, *Icarus* **109**, 156 (1994).
 26. S. C. Solomon, *Geophys. Res. Lett.* **5**, 461 (1978); H. J. Melosh and W. B. McKinnon, in (2), p. 374.
 27. The uniqueness of Mercury in this context is simply due to its proximity to the sun: unlike Earth and Venus, a large fraction of Mercury's mantle excavated during the giant impact falls into the sun rather than reaccumulating, thus explaining the anomalously thin mantle and the resulting sluggish convection (low Rayleigh number) within the planet (11, 12). With sublithosphere mantle thicknesses of 400 km, 1100 km, and 2750 km for Mercury, the moon, and Earth (10), respectively, scaling arguments yield Rayleigh numbers reduced by ~2.5 and ~1.2 orders of magnitude for Mercury and the moon relative to Earth [R. Jeanloz and S. Morris, *Annu. Rev. Earth Planet. Sci.* **14**, 377 (1986)]. Low Rayleigh numbers, barely higher than the critical value defining the onset of convection, are also found in detailed calculations of Mercury's thermal evolution (7).
 28. D. W. Hyndman, *Petrology of Igneous and Metamorphic Rocks* (McGraw-Hill, New York, ed. 2, 1982).
 29. The Schrödinger Basin area was described by E. M. Shoemaker, M. S. Robinson, and E. M. Eliason [*Sci-*

ence **266**, 1851 (1994)]. Observations and scaling relations indicate that the volume of shock-induced melt increases rapidly with increasing impact energy and crater size [R. A. F. Grieve and M. J. Cintala, *Meteoritics* **27**, 526 (1992); *ibid.* **28**, 602 (1993)], suggesting that impact-melt units could be more abundant on Mercury's surface than previously recognized [see (1–3)].

30. M. J. Campbell and J. Ulrichs, *J. Geophys. Res.* **74**, 5867 (1969).
31. Both of these assumptions are conservative in that scattering losses can only increase the microwave opacity from the value determined by the intrinsic

dielectric loss at a given frequency (15). Also, a regolith density of 1.5 g/cm³ is in the low range of lunar values (20); assuming a higher density for Mercury's regolith would require an even lower dielectric loss tangent to compensate. Thus, our values in Fig. 2 may overestimate the intrinsic dielectric loss tangent of Mercury's surface.

32. We thank I. Carmichael and E. Shoemaker for helpful comments. This work was supported by the National Aeronautics and Space Administration and the National Science Foundation.

4 November 1994; accepted 6 March 1995

Single Molecule Electron Paramagnetic Resonance Spectroscopy: Hyperfine Splitting Owing to a Single Nucleus

J. Köhler, A. C. J. Brouwer, E. J. J. Groenen, J. Schmidt*

Individual pentacene-*d*₁₄ molecules doped into a *p*-terphenyl-*d*₁₄ host crystal have been studied by optically detected electron paramagnetic resonance spectroscopy. The magnetic resonance transitions between the triplet sublevels of the pentacene molecule and the splitting of the resonance lines for a molecule that contains a carbon-13 nucleus have been observed in an external magnetic field. This splitting is caused by the hyperfine interaction of the triplet electron spin with the single carbon-13 nuclear spin.

In recent years, the feasibility of using spectroscopy in the condensed phase on the level of a single molecule has been demonstrated (1, 2). As a result, studies free from the averaging over molecular ensembles that is inherent to conventional spectroscopy became possible, and phenomena such as spectral diffusion (3–5), photon bunching (2, 6), and antibunching (7) have been made visible. Meanwhile, a wealth of experimental techniques have been applied to single molecules in various environments (8). In addition, the optical detection of single molecules has been combined with magnetic resonance techniques to make possible the detection of the triplet sublevel transitions of a single pentacene molecule in a *p*-terphenyl host (9, 10). The broadening of the triplet transitions owing to the interaction of the single triplet electron spin with a single ¹³C nucleus has been observed through the selective excitation of a pentacene molecule containing a ¹³C nucleus at a particular position (11). With this contribution we really enter the domain of magnetic resonance spectroscopy, and we report here the observation of a single triplet electron spin in an external magnetic field.

Thin, sublimation-grown crystals of *p*-terphenyl-*d*₁₄ containing about 10⁻⁸ mol of pentacene-*d*₁₄ per mole of *p*-terphenyl-*d*₁₄

were cooled to 1.2 K. As described in detail in (11), the crystals were mounted between a LiF substrate and a quartz cover in the joint focus of a lens and a parabolic mirror. Even for these high-quality crystals, the S₁ ← S₀ transition of pentacene is inhomogeneously broadened owing to the slight differences in the local environments of the guest molecules. Exciting the system by a single-mode laser tuned into the wing of this transition, where the density of absorbers per unit frequency is low, allows the detection of single molecules. The fluorescence emitted to the red of the absorption is collected by the parabolic mirror and recorded by a photomultiplier and photon counting. When the molecule is excited into the S₁ singlet state, it can escape from the S₀ ↔ S₁ excitation-emission cycle to the lowest triplet state T₁ with a probability of 0.5%. Consequently, the fluorescence photons are emitted in bunches with an average dark period that corresponds to the mean residence time of the molecule in the triplet state. The three sublevels of T₁, labeled T_x, T_y, and T_z, are selectively populated and depopulated by intersystem crossing. Because levels T_x and T_y have a short lifetime and a high population probability compared to level T_z (12), the mean residence time of a molecule in the triplet state is prolonged under the influence of a microwave field in resonance with the (T_x-T_z) or (T_y-T_z) transition. This allows the observation of these magnetic resonance transitions as a decrease in fluorescence [fluorescence-detected magnetic reso-

Center for the Study of Excited States of Molecules, Huygens Laboratory, University of Leiden, Post Office Box 9504, 2300 RA Leiden, Netherlands.

*To whom correspondence should be addressed.

nance (FDMR)]. In order to do this, the laser is tuned to the peak of the absorption line of a single molecule. A small grounded loop close to the sample provides for a microwave field that is on-off-modulated at 37 Hz. The microwaves are generated by a microwave sweeper that is stabilized to within 5 kHz by a frequency counter and a software feedback loop. The stabilized frequency is stepped with a typical dwell time of 4 s, and the difference in the number of photons counted during the "microwave-on" and the "microwave-off" periods is recorded. The FDMR spectra are obtained by averaging over a number of these stepped frequency scans. For the experiment in an external magnetic field, the sample holder is inserted in a superconducting magnet.

The $S_1 \leftarrow S_0$ fluorescence-excitation spectrum of pentacene in *p*-terphenyl shows four distinct, inhomogeneously broadened zero-phonon lines labeled O_1 to O_4 in order of increasing absorption frequency. These correspond to the four inequivalent sites in the *p*-terphenyl host crystal that can be occupied by pentacene (13). Magnetic resonance transitions have been optically detected in zero field for O_1 and O_2 pentacene molecules, both for ensembles and for single molecules (9, 10, 12, 14). The results obtained for O_1 and O_2 are equivalent, apart from a slight shift of the (T_x - T_z) and (T_y - T_z) transitions. Both triplet transitions show a considerable, asymmetric broadening caused by the hyperfine interaction of the triplet electron spin with the surrounding proton nuclear spins (9, 12). In order to reduce this effect for the present experiments, the protons of the guest and the host

molecules are replaced by deuterium. This leads to a drastic decrease of the linewidth (Fig. 1). The figure compares the (T_x - T_z) transition for an ensemble of O_1 molecules for a pentacene- h_{14} (Fig. 1A) and a pentacene- d_{14} (Fig. 1B) sample. The nuclear magnetic moment of deuterium is about 15% of that of the proton, which reduces the linewidth by a factor of about 40 because the hyperfine interaction is a second-order effect in zero external magnetic field. The width of 120 kHz in Fig. 1B corresponds to the limit of low microwave power.

The isotopic substitution of deuterium for hydrogen also leads to a shift of the optical absorption toward higher frequency caused by a decrease of vibrational energies and, consequently, of zero-point energies in the ground state and to a lesser extent in the excited electronic state. The optical absorption of pentacene- d_{14} is shifted by 32.8 cm^{-1} for O_1 and by 34.5 cm^{-1} for O_2 relative to that of pentacene- h_{14} . In Fig. 2A, the O_1 spectral region of the fluorescence-

excitation spectrum of pentacene- d_{14} in *p*-terphenyl- d_{14} is shown. The absorption at $(16,915.529 \pm 0.003) \text{ cm}^{-1}$ has a linewidth of 0.085 cm^{-1} (2.5 GHz) and is accompanied by a weak satellite structure at higher energies. The shift of satellites 1, 2, and 3 with respect to the main line amounts to 0.30 cm^{-1} , 0.49 cm^{-1} , and 0.62 cm^{-1} , respectively, in close agreement with the shifts observed for pentacene- h_{14} molecules containing single ^{13}C nuclei (11, 15). By analogy with our earlier study (11), we assign the main line to pentacene- d_{14} containing exclusively ^{12}C (with a probability of 78.8% given the 1.108% natural abundance of ^{13}C), and we assign the satellites to deuterated pentacene molecules containing a single ^{13}C nucleus in position α or δ (satellite 1), ϵ (satellite 2), and γ (satellite 3) (see Fig. 3). Lines corresponding to ^{13}C nuclei in other positions, which we observed for pentacene- h_{14} in *p*-terphenyl- h_{14} , are not resolved here because of the inhomogeneous linewidth of 2.5 GHz, which causes these satellites to be hidden under the wing of the main line.

The fluorescence-excitation spectrum in Fig. 2A suggests that single molecules without ^{13}C are most likely to be encountered to the red of the main line, whereas single molecules containing a ^{13}C nucleus should be abundant to the blue of satellite 3. In Fig. 2, B and C, the (T_x - T_z) magnetic resonance transitions of two different molecules in zero magnetic field are shown. The single-molecule FDMR spectra were recorded with a microwave power 100 times that used for the spectrum in Fig. 1B. For molecule I, which most probably contains only ^{12}C nuclei, a magnetic resonance transition with a linewidth of 670 kHz was observed. We attribute this broadening to saturation because a similar linewidth is obtained for the ensemble spectrum if it is recorded with the same microwave power. For molecule II, which contains a ^{13}C nucleus, the width of the magnetic resonance transition amounts to 4.8 MHz and the transition is shifted by 6 MHz toward higher energy compared to that for molecule I. The shift is due to the interaction of the triplet electron spin with a single ^{13}C nuclear spin in position γ of the pentacene molecule.

The hyperfine interaction, second-order in zero field, can be approximated by perturbation theory. For a single nucleus, this results in a negligible shift of the T_z level,

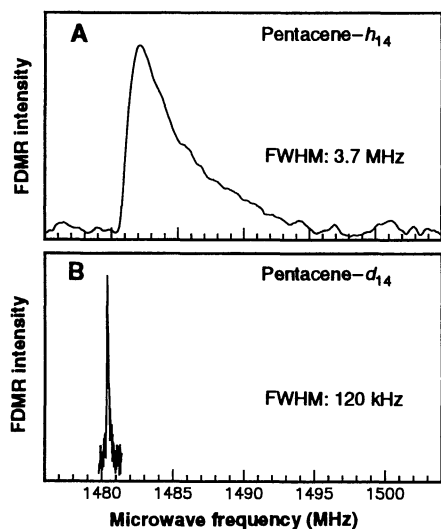


Fig. 1. Comparison of the line shape of the (T_x - T_z) magnetic resonance transition in zero field for an ensemble of molecules for (A) pentacene- h_{14} in *p*-terphenyl- h_{14} and (B) pentacene- d_{14} in *p*-terphenyl- d_{14} . The signals correspond to a decrease of the fluorescence. The full width at half maximum (FWHM) for each line is given in the figure.

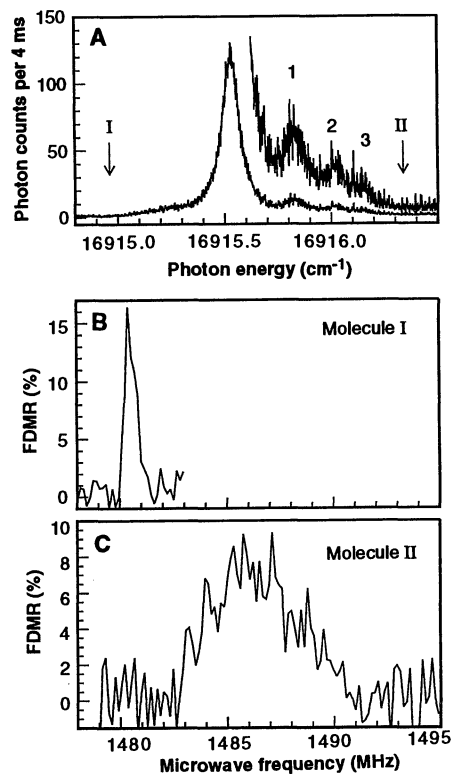


Fig. 2. (A) Fluorescence-excitation spectrum of the O_1 spectral region for pentacene- d_{14} in *p*-terphenyl- d_{14} . The incident laser power was 70 mW cm^{-2} . The scale is valid for the lower trace; for the upper trace, the spectrum has been multiplied by 5. The "noisy" structure of the spectrum results from statistical fine structure (SFS) (18). Arrows indicate the spectral positions of molecules I and II. (B) Fluorescence-detected magnetic resonance transition (T_x - T_z) for molecule I in zero field and (C) for molecule II in zero field. The vertical scale in (B) and (C) represents the relative decrease of the fluorescence.

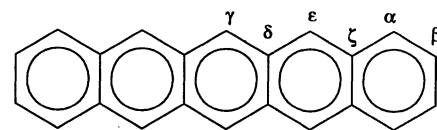


Fig. 3. Schematic representation of the pentacene molecule with the labeling of the carbon positions.

whereas the shift of the T_x level is given by $\frac{1}{4}\rho_i^2 A_{zz}^2 / (E_x - E_y)$, where ρ_i represents the spin density in the $2p_z$ orbital of carbon number i , A_{zz} is the z component of the hyperfine-interaction tensor of the nucleus (that is, ^{13}C at position i or ^2H bound to the carbon in position i), and $(E_x - E_y)$ is the energy difference between the triplet sub-levels T_x and T_y . For a (hypothetical) spin density of 1 at a certain carbon atom, this would cause a shift of about 200 MHz owing to a ^{13}C in that position and a shift of about 190 kHz owing to a ^2H . Hence, the ^{13}C hyperfine interaction is by far the more dominant shift and leads to a shift of the zero-field transition whereas the distribution of the 14 ^2H nuclei over all possible spin states modulates this shift and thereby broadens the line. Using the known spin-density distribution (16), we estimate a shift

of the (T_x-T_z) transition of 7 MHz for a ^{13}C nucleus in one of the two center positions (γ) of the pentacene molecule, which is in agreement with the observed shift. The present situation is essentially different from the pentacene- h_{14} case, for which the hyperfine interaction with the 14 proton spins is sufficient to compensate the ^{13}C contribution and only an asymmetric broadening rather than a shift of the transition is observed (11).

Upon application of external magnetic fields up to 7.5 mT, a shift, broadening, or splitting of the (T_x-T_z) and (T_y-T_z) transitions has been observed as illustrated for the (T_x-T_z) transition of three different molecules in Fig. 4. Molecules I and II are O_1 molecules, whereas molecule III is an O_2 molecule excited to the blue of the O_2 zero-phonon line; molecule I consists completely of ^{12}C nuclei, whereas molecules II and III contain a ^{13}C nucleus in position γ . The magnetic field leads to a mixing of the zero-field states T_x , T_y , and T_z , and the proper eigenstates of the system are found by diagonalization of the spin Hamiltonian, which includes the zero-field and the electronic Zeeman interaction. They can be expressed as linear combinations of the zero-field states. The coefficients of the linear combinations are determined by the strength of the applied magnetic field and its orientation with respect to the molecule. Because only weak magnetic fields have been used in this study, we will still refer to the triplet substances by their zero-field labels.

From the analysis of the magnetic field-induced shifts of the (T_x-T_z) and (T_y-T_z) transition for O_1 , we have obtained the orientation of the magnetic field with respect to these pentacene molecules. Orientations as deduced from ensemble and several single-molecule experiments did not differ significantly (experimental accuracy $\pm 5^\circ$). Tuning the laser into resonance with the O_2 zero-phonon transition allowed a similar study for the O_2 molecules. If we assume that the pentacene molecules in the

host crystal are oriented like the p -terphenyl molecules they replace, the different field-induced shifts observed for the magnetic resonance transitions of O_1 and O_2 pentacene molecules lead us to conclude that these occupy lattice sites with a significantly different orientation. The p -terphenyl molecules in lattice sites P_1 to P_4 can be grouped into two pairs (P_1 and P_2) and (P_3 and P_4) such that the p -terphenyl molecules within a pair are oriented nearly parallel with respect to each other, whereas the molecules from different groups are rotated with respect to each other about the long axis of the molecule by roughly 60° (13). Consequently, only the combinations of lattice sites (P_1 and P_3), (P_1 and P_4), (P_2 and P_3), and (P_2 and P_4) can be occupied by those pentacene molecules responsible for the (O_1 and O_2) zero-phonon lines. The combination (P_3 and P_4) for (O_1 and O_2) as given in (17) can be ruled out.

The FDMR spectra for molecule I (Fig. 4A) show a shift of the magnetic resonance transition and a broadening of the line in the magnetic field. The shift results from the electronic Zeeman interaction, whereas the broadening is caused by the hyperfine interaction with the 14 ^2H nuclear spins. Figure 4B shows the FDMR spectra of molecule II. Besides a frequency shift of the transition similar to that observed for molecule I, the magnetic resonance transition of molecule II splits into two components. We assign this splitting to the hyperfine interaction of the triplet electron spin with the single ^{13}C nuclear spin. For molecule III (Fig. 4C), both the observed shift and the splitting of the magnetic resonance transition are different from those obtained for the O_1 molecules owing to the different orientation of O_2 and O_1 molecules with respect to the magnetic field. Using a spin Hamiltonian that takes into account the zero-field splitting, the electronic Zeeman interaction, and the ^{13}C hyperfine interaction, and using the known orientation of the magnetic field with respect to the mol-

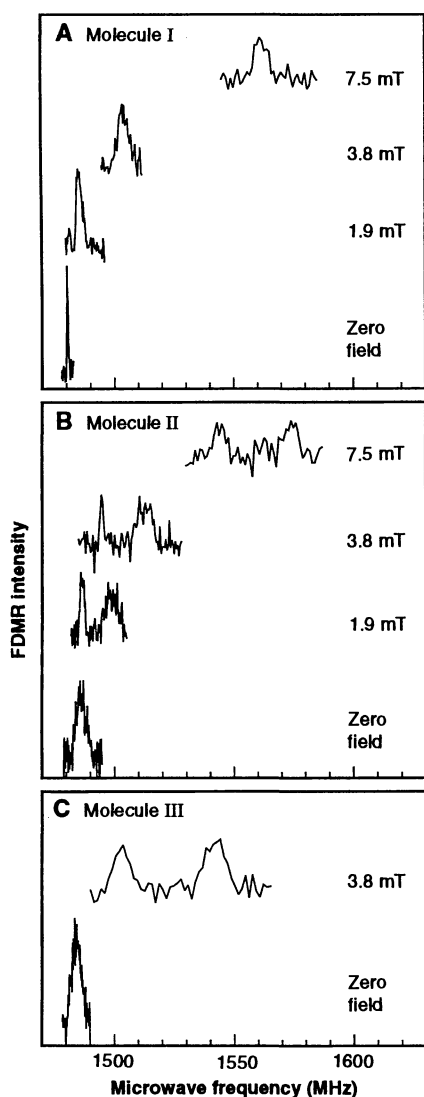


Fig. 4. Fluorescence-detected magnetic resonance transition (T_x-T_z) (A) for molecule I, (B) for molecule II, and (C) for molecule III in weak magnetic fields. The scales of spectra (A), (B), and (C) are different.

Table 1. Comparison of the calculated and observed hyperfine splitting for various molecules. The O_1 and O_2 molecules were identified by their different zero-field frequencies. The labels ε and γ refer to the position of the ^{13}C nucleus in pentacene (see Fig. 3).

Molecule (type)	^{13}C position	Field (mT)	Splitting (MHz)	
			Observed	Calculated
II (O_1)	γ	1.9	12.3	11.2
		3.8	18.0	20.7
		7.5	30.0	31.9
III (O_2)	γ	3.8	39.0	43.8
IV (O_1)	γ	3.8	19.0	20.7
V (O_1)	γ	3.8	19.0	20.7
VI (O_1)	ε	1.9	7.6	8.0
		3.4	11.0	13.4
VII (O_2)	γ	3.8	39.0	43.8
VIII (O_2)	γ	3.4	42.0	41.8

ecule under study, we have calculated the frequencies of the four possible transitions for various molecules. Two pairs of close-lying lines result, and the calculated hyperfine splitting between these pairs (Table 1) agrees well with the experimental values given the underlying approximations.

Interestingly, both hyperfine components show up in the FDMR spectra, as is clear for molecules II and III in Fig. 4, in spite of the fact that we study single quantum systems. Apparently the triplet spin experiences both ^{13}C nuclear spin configurations during the time (about 30 min) needed to accumulate the spectra. When the pentacene molecule is in S_0 , the ^{13}C nuclear spin can undergo energy conserving flip-flop transitions caused by the dipole-dipole interaction with other ^{13}C nuclei. If the mean distance between two ^{13}C nuclei is of the order of 10 nm, a rough estimate of this flip-flop time is 1 to 10 s, which is short relative to the accumulation time. We therefore observe a time average that is equivalent to the ensemble average according to the ergodic theorem.

For very small magnetic fields, the widths of the two hyperfine components for molecule II differ (see Fig. 4B). Each of the hyperfine components is built up by two transitions merged into one line. The width is caused by the hyperfine interaction with the 14 ^2H nuclear spins. A calculation of this interaction shows that for O_1 molecules in very low fields the mixing of zero-field states is such that the second-order hyperfine interaction determines the linewidth of the low-frequency hyperfine component, whereas the first-order hyperfine interaction dominates for the high-frequency component. For a magnetic field of 7.5 mT, the hyperfine interaction becomes totally first-order and a more symmetrical pattern results. As seen for molecule III in Fig. 4C, this is already true at 3.8 mT for an O_2 molecule owing to the different orientation of the molecule with respect to the magnetic field.

REFERENCES AND NOTES

- W. E. Moerner and L. Kador, *Phys. Rev. Lett.* **62**, 2535 (1989).
- M. Orrit and J. Bernard, *ibid.* **65**, 2716 (1990).
- W. P. Ambrose and W. E. Moerner, *Nature* **349**, 225 (1991).
- W. P. Ambrose, Th. Basché, W. E. Moerner, *J. Chem. Phys.* **95**, 7150 (1991).
- A. Zumbusch, L. Fleury, R. Brown, J. Bernard, M. Orrit, *Phys. Rev. Lett.* **70**, 3584 (1993).
- J. Bernard, L. Fleury, H. Talon, M. Orrit, *J. Chem. Phys.* **98**, 850 (1993).
- Th. Basché, W. E. Moerner, M. Orrit, H. Talon, *Phys. Rev. Lett.* **69**, 1516 (1992).
- W. E. Moerner and Th. Basché, *Angew. Chem. Int. Ed. Engl.* **32**, 457 (1993); M. Orrit, J. Bernard, R. I. Personov, *J. Phys. Chem.* **97**, 10256 (1993); W. E. Moerner, *Science* **265**, 46 (1994); A. B. Myers, P. Tchénio, M. Z. Zgierski, W. E. Moerner, *J. Phys. Chem.* **98**, 10377 (1994).
- J. Köhler *et al.*, *Nature* **363**, 242 (1993).
- J. Wrachtrup, C. von Borczyskowski, J. Bernard,

- M. Orrit, R. Brown, *ibid.*, p. 244.
- J. Köhler, A. C. J. Brouwer, E. J. J. Groenen, J. Schmidt, *Chem. Phys. Lett.* **228**, 47 (1994).
- J. Wrachtrup, C. von Borczyskowski, J. Bernard, M. Orrit, R. Brown, *Phys. Rev. Lett.* **71**, 3565 (1993).
- P. J. L. Baudour, Y. Delugeard, H. Cailleau, *Acta Crystallogr. Sect. B* **32**, 150 (1976).
- R. Brown, J. Wrachtrup, M. Orrit, J. Bernard, C. von Borczyskowski, *J. Chem. Phys.* **100**, 7182 (1994).
- Th. Basché, S. Kummer, C. Bräuchle, *Chem. Phys. Lett.* **225**, 116 (1994).
- T. T. Lin, J. L. Ong, D. J. Sloop, H. L. Yu, in *Pulsed EPR: A New Field of Applications*, C. P. Keijzers, E. J. Reijerse, J. Schmidt, Eds. (North-Holland, Amsterdam, 1989), p. 191.
- H.-C. Fleischhauer, C. Kryschi, B. Wagner, H.

- Kupka, *J. Chem. Phys.* **97**, 1742 (1992); C. Kryschi, H.-C. Fleischhauer, B. Wagner, *Chem. Phys.* **161**, 485 (1992).
- SFS denotes the spectral roughness caused by the static, statistical number fluctuations of the emitting molecules.
- We thank H. Zimmermann and H.-M. Vieth for providing pentacene- d_{14} . This work is supported by the Stichting voor Fundamenteel Onderzoek der Materie (FOM), with financial aid from the Nederlandse Organisatie voor Wetenschappelijk Onderzoek (NWO). One of us (J.K.) is fellow of the Human Capital and Mobility program of the European Community (grant ERBCHBICT920190).

2 February 1995; accepted 27 March 1995

Electronic States in Gallium Arsenide Quantum Wells Probed by Optically Pumped NMR

R. Tycko,*† S. E. Barrett,*‡ G. Dabbagh, L. N. Pfeiffer, K. W. West

An optical pumping technique was used to enhance and localize nuclear magnetic resonance (NMR) signals from an n -doped $\text{GaAs}/\text{Al}_{0.1}\text{Ga}_{0.9}\text{As}$ multiple quantum well structure, permitting direct radio-frequency measurements of gallium-71 NMR spectra and nuclear spin-lattice relaxation rates ($1/T_1$) as functions of temperature ($1.6\text{ K} < T < 4.2\text{ K}$) and the Landau level filling factor ($0.66 < \nu < 1.76$). The measurements reveal effects of electron-electron interactions on the energy levels and spin states of the two-dimensional electron system confined in the GaAs wells. Minima in $1/T_1$ at $\nu \approx 1$ and $\nu \approx 2/3$ indicate energy gaps for electronic excitations in both integer and fractional quantum Hall states. Rapid, temperature-independent relaxation at intermediate ν values indicates a manifold of low-lying electronic states with mixed spin polarizations.

Electrons in two-dimensional (2D) systems exhibit striking physical phenomena that are not observed in conventional 3D materials, particularly at low temperatures and in high magnetic fields. These phenomena include the integer quantum Hall effect (IQHE) and the fractional quantum Hall effect (FQHE) (1). The clearest realization of a 2D electron system (2DES) is provided by the conduction electrons in high-mobility semiconductor quantum wells, that is, thin layers of one semiconductor (here GaAs) embedded in thicker layers of a second n -doped semiconductor with a larger band gap (here delta-doped $\text{Al}_{0.1}\text{Ga}_{0.9}\text{As}$). Because of the band gap differences, the GaAs layers act as potential energy wells for the doped electrons and the $\text{Al}_{0.1}\text{Ga}_{0.9}\text{As}$ layers act as potential barriers. At low temperatures ($T \ll 100\text{ K}$), where only the lowest two dimensionally confined electron subband is populated, and in the absence of electron-electron interactions, the electronic properties of an ideal n -doped quan-

tum well in a magnetic field B can be understood in terms of the single-particle energy level diagram in Fig. 1 (2). The translational energy is quantized in Landau levels with splittings equal to the cyclotron energy $E_c = \hbar e B_z / m^* c$, where \hbar is Planck's constant h divided by 2π , e is the electron charge, B_z is the component of the field normal to the plane of the wells, m^* is the effective electron mass, and c is the speed of light. The Landau levels are further split by the electron spin Zeeman energy $E_Z = g^* \mu_B |B|$, where g^* is the effective g value and μ_B is the Bohr magneton. Each energy level has well-defined values of the orbital ($N = 0, 1, 2, 3, \dots$) and spin ($m = \pm 1/2$) quantum numbers and is highly degenerate, with degeneracy per unit area $n_B = e B_z / hc$. The Landau level filling factor is then defined as $\nu = n_s / n_B$, where n_s is the conduction electron density per unit area in a single well, so that ν represents the number of spin-split Landau levels that are occupied at $T = 0$. The IQHE and FQHE refer to characteristic and universal plateaus in the Hall resistance and zeros in the longitudinal resistance of a 2DES at integral and certain fractional values of ν . These effects, and other postulated phenomena such as Wigner crystallization, depend on deviations from the simple picture in Fig. 1

AT&T Bell Laboratories, 600 Mountain Avenue, Murray Hill, NJ 07974, USA.

*To whom correspondence should be addressed.

†Present address: National Institutes of Health, Building 5, Room 112, Bethesda, MD 20892, USA.

‡Present address: Department of Physics, Yale University, New Haven, CT 06520, USA.